Physics and Imaging in Radiation Oncology 16 (2020) 81–84

Contents lists available at ScienceDirect

Physics and Imaging in Radiation Oncology

journal homepage: www.sciencedirect.com/journal/physics-and-imaging-in-radiation-oncology

Short Communication

Dose response of three-dimensional silicone-based radiochromic dosimeters for photon irradiation in the presence of a magnetic field☆

Morten B. Jensen [a,b,*], Peter Balling [c,d], Simon J. Doran [e], Jørgen B.B. Petersen [b], Isak H. Wahlstedt [f,g,h], Ludvig P. Muren [a,b]

[a] Danish Centre for Particle Therapy, Aarhus University Hospital, Aarhus, Denmark
[b] Department of Medical Physics, Aarhus University Hospital, Aarhus, Denmark
[c] Department of Physics and Astronomy, Aarhus University, Aarhus, Denmark
[d] Interdisciplinary Nanoscience Center, Aarhus University, Aarhus, Denmark
[e] The Institute of Cancer Research, London, UK
[f] Technical University of Denmark, Lyngby, Denmark
[g] Department of Clinical Oncology, Rigshospitalet, Copenhagen, Denmark
[h] Department of Oncology, Herlev and Gentofte Hospital, Copenhagen, Denmark

ARTICLE INFO

Keywords:
3D radiation dosimetry
Magnetic resonance imaging guided radiotherapy

ABSTRACT

The magnetic field in magnetic resonance imaging guided radiotherapy (MRgRT) delivery systems influences charged-particle trajectories and hence the three-dimensional (3D) radiation dose distributions. This study investigated the dose-response as well as dose-rate and fractionation dependencies of silicone-based 3D radiochromic dosimeters for photon irradiation in a magnetic field using a 0.35 T MRgRT system. We found a linear dose response up to 22.6 Gy and no significant dose-rate dependency as a function of depth. A difference in optical response was observed for dosimeters irradiated in a single compared to multiple fractions. The dosimeter showed clinical potential for verification of MRgRT delivery.

1. Introduction

The strong magnetic field of magnetic resonance imaging guided radiotherapy (MRgRT) systems influences the motion of charged particles and causes changes in the patterns of dose deposition in three dimensions (3D) [1]. Current dosimeters and techniques of quality assurance used for conventional radiotherapy therefore have to be adjusted to be applicable for MRgRT systems [2]. Ionization-chamber correction factors for reference dosimetry in MRgRT systems have been validated [3], while radiochromic films show no significant changes in optical density due to the presence of a magnetic field [4,5]. These techniques, however, are limited to point and planar measurements.

Several methods have been developed over the past years to allow for 3D dose measurements [6–8]. Dosimeters such as PRESAGE® (radiochromic plastic), FOX (radiochromic gel), BANG (polymer gel), and others have been investigated in the presence of a magnetic field and have been shown to be applicable for MRgRT systems [1].

A new deformable silicone-based radiochromic 3D dosimeter has been proposed and has already been assessed in the *absence* of a magnetic field in terms of dosimetric and mechanical properties as well as dose-rate dependency, with promising results for both photon and proton beams [9–14]. The dosimeter can potentially be moulded into 3D anthropomorphic phantoms and complex phantom geometries including air-tissue interfaces. Such interfaces are of special interest for MRgRT systems due to the electron-return effects (ERE) [15]. The aim of the present study was to assess the potential of this dosimeter for MRgRT systems by characterizing its key properties in the presence of a magnetic field.

☆ Dr. Ludvig Muren, a co-author of this paper, is an Editor-in-Chief of Physics & Imaging in Radiation Oncology. The editorial process for this manuscript was managed independently from Dr. Muren and the manuscript was subject to the Journal's usual peer-review process.

* Corresponding author.
E-mail address: mobjje@rm.dk (M.B. Jensen).

https://doi.org/10.1016/j.phro.2020.10.003
Received 2 July 2020; Received in revised form 2 October 2020; Accepted 5 October 2020
Available online 19 October 2020

2. Material and methods

2.1. Fabrication

Dosimeters were fabricated from silicone elastomer (SE), curing agent (CA), chloroform and leuco-malachite green (LMG). The SE and CA came from the commercially available SYLGARD 184 Silicone Elastomer (DOW) Kit. The batches were fabricated with 0.26% (w/w) LMG dissolved in 1.5% (w/w) chloroform and then mixed with 89.2% (w/w) SE and 9% (w/w) CA using a mixer. Air bubbles were removed using a vacuum desiccator before the mixture was poured into polystyrene cuvettes (1 cm × 1 cm × 4.5 cm) and left to cure protected from light at room temperature. Two batches of dosimeters were used in this study and they were fabricated approx. 55 h (batch one) and 45 h (batch two) prior to irradiation, respectively, based on our previous characterization of the dosimeter response versus composition and curing time [9,10].

2.2. Irradiation conditions

All dosimeters were irradiated using the MRIdian MRgRT system (ViewRay Inc., USA) at Herlev Hospital, Herlev, Denmark, with a magnetic field strength of 0.35 T, a 10 × 10 cm^2 field, 6 MV beam quality, flattening-filter-free mode, a source-to-isocentre distance of 90 cm and a dose rate of 650 monitor units (MU)/min (all parameters were fixed by manufacturer except the field size). The number of MU given for a specific dose was calculated on a virtual water phantom in the treatment planning system and the beam output was within the tolerance of clinical use for patient treatments. For all irradiations, five dosimeters were irradiated at the same time.

The dose response was measured in 10 cm depth by placing the dosimeters between a 5 cm solid water (SW) backscatter slab and a 9.5 cm SW build-up slab. The dosimeters were centered in the radiation field with a source-to-surface distance (SSD) of 80 cm and irradiated with an approx. dose rate of 4.9 Gy/min to total doses of 1.5, 3.8, 7.5, 11.3, 15.1, 18.9 and 22.6 Gy.

For the depth dose-rate measurements, the dosimeters were irradiated in depths of 5, 10 and 15 cm with a constant SSD of 85 cm. For 5 cm depth, the dosimeters were placed between a 5 cm SW backscatter slab and 4.5 cm SW build up slab. Measurement depths of 10 and 15 cm were obtained by placing additional 5 cm SW slabs while adjusting the treatment couch to maintain an SSD of 85 cm. Each beam was delivered with an approx. dose rate of 650 MU/min corresponding to approx. dose rates during field delivery of 6.0, 4.5 and 3.3 Gy/min at depths 5, 10 and 15 cm respectively.

For the fractionation measurements, the setup was identical to the one used for the dose-response experiments. A total dose of 7.5 Gy was delivered in 1, 2, 4 and 10 fractions with a total beam delivery time of approx. 100 s. The fractionated doses were delivered in a total treatment time of 6.5 min at regular time intervals i.e. the time between fractions was kept constant for each fractionation. The total treatment time for the single-fraction irradiation was approx. 100 s.

Dosimeters used in the dose-response and fractionation experiments were made from batch one and dosimeters used for the depth dose-rate experiments were made from batch two.

2.3. Pre- and post-irradiation optical read-out and data analysis

The difference in optical density before and after irradiation ($\Delta OD_{irradiated}$) for each dosimeter was measured using a spectrophotometer (Spectroquant Pharo 100). The dosimeters were measured at approx. 625 nm, which is close to the absorption peak for the present chemical composition [10]. The dosimeters were pre-scanned approx. 20 h before irradiation and post-scanned approx. 6 h after irradiation.

For both batches, zero-dose reference dosimeters were brought back and forth to the irradiation source under the same conditions as the irradiated dosimeters, and they were pre- and post-scanned at the same time. The difference in optical density ($\Delta OD_{zero\text{-}dose}$) was calculated.

ΔOD was defined as the mean value of $\Delta OD_{zero\text{-}dose}$ for the batch in question subtracted from $\Delta OD_{irradiated}$ for each individual dosimeter. The optical response, $\Delta\alpha$, was calculated as ΔOD divided by the optical path length (1 cm) and was plotted against dose and fitted with a linear regression with the slope being the dose response.

For statistical analysis, the normality of data as well as the hypotheses of common variance were evaluated, following detailed description of statistical analysis. For the depth dose-rate experiments, the hypothesis of identical slopes was tested by comparing the regression line at each depth with the others [16]. The data for the fractionation experiments was analysed using one-way analysis of variance.

3. Results

We found a dose response (including 95% confidence interval) of $(13.2 \pm 0.2) \times 10^{-3}$ cm^{-1} Gy^{-1} (Fig. 1). The dose responses at different depths were $(14.2 \pm 0.3) \times 10^{-3}$ cm^{-1} Gy^{-1} at 5 cm, $(14.4 \pm 0.4) \times 10^{-3}$ cm^{-1} Gy^{-1} at 10 cm, and $(14.3 \pm 0.3) \times 10^{-3}$ cm^{-1} Gy^{-1} at 15 cm (Fig. 2). Comparison of regression lines in the depth dose-rate experiment did not reject the hypothesis of identical slopes with p-values of 0.26, 0.51 and 0.63.

For the fractionation experiment at 7.5 Gy, we found a mean (and 95% confidence interval) of the optical response of $(103.9 \pm 3.2) \times 10^{-3}$ cm^{-1} for 1 fraction, $(97.5 \pm 3.4) \times 10^{-3}$ cm^{-1} for 2 fractions, $(97.1 \pm 3.4) \times 10^{-3}$ cm^{-1} for 4 fractions and $(99.1 \pm 4.0) \times 10^{-3}$ cm^{-1} for 10 fractions. One-way analysis of variance rejected the hypothesis of equal means ($p = 0.006$) between all four groups.

The mean changes in attenuation of the zero-dose dosimeters were $(28.1 \pm 0.5) \times 10^{-3}$ cm^{-1} and $(22.2 \pm 0.5) \times 10^{-3}$ cm^{-1} for batch one (16 dosimeters) and two (14 dosimeters), respectively. The mean values of the associated pre-scans were $(198.4 \pm 2.4) \times 10^{-3}$ cm^{-1} and $(188.9 \pm 2.2) \times 10^{-3}$ cm^{-1}.

4. Discussion

In the presence of a magnetic field, our radiochromic dosimeters showed a linear dose response up to 22.6 Gy and no significant variation in dose response as a function of depth with effective dose rates ranging from approx. 3.3 to 6.0 Gy/min. A difference in optical response for a dose delivered in one single fraction compared to in multiple fractions

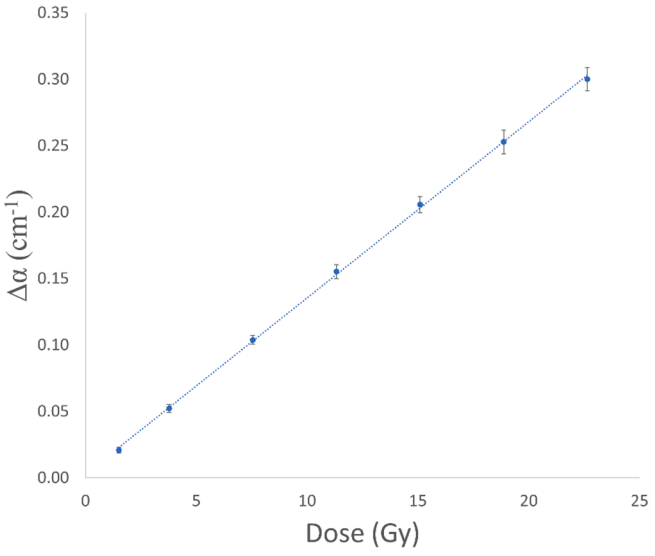

Fig. 1. Optical response as a function of dose. The error bars represent the 95% confidence interval of the five observations in each group. $R^2 > 0.99$ for the regression model. Dosimeters were made from batch one.

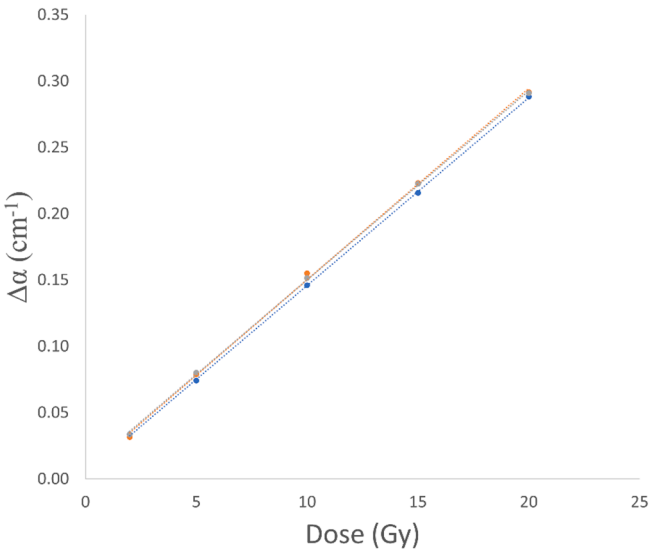

Fig. 2. Optical response as a function of dose for depths of 5 cm (blue), 10 cm (orange) and 15 cm (grey). The error bars on the data points are roughly the size of the marker and have been omitted for clarity. $R^2 > 0.99$ for all three regression models. Dosimeters were made from batch two.

was observed.

The dose-response experiment showed a dose response of 13.2×10^{-3} cm^{-1} Gy^{-1}, whereas the depth dose-rate experiment showed a dose response of approx. 14.3×10^{-3} cm^{-1} Gy^{-1}. The small difference in dose response is attributed to the experiments being done with two different batches with time interval between fabrication and irradiation differing by 10 h. The difference in storage time as well as in the thermal and light-exposure history can affect the dose response [10,17]. In a previous study (irradiations without a magnetic field), we found a dose response in the same range, also comparable to the dose response of PRESAGE® [9,18]. No significant dose-rate dependency as a function of depth was observed which was also demonstrated previously in the absence of a magnetic field [10].

For the fractionation experiment, the optical response for 7.5 Gy delivered in one single fraction was higher with a relative difference up to about 7% compared to multiple fractions. The single-fraction irradiation was carried out approx. 1 h before the others (measurements done in connection with dose-response experiment), which potentially could have an influence. However, the outcome matched previous results without a magnetic field, where we found Δα for fractionated irradiations 5–11% lower compared to a single fraction with total dose of 30 Gy given in 15 min [10]. It is an important characteristic to investigate for the dosimeter to work as a good integrating dosimeter and for validation of treatment plans with spatially overlapping fields.

The dose-response and fractionation measurements were done with SSD = 80 cm and the depth dose-rate measurements were done with SSD = 85 cm. Since the dose rate for the dose-response and fractionation experiments was within the dose-rate range investigated in the depth dose-rate experiment (where no significant variation of dose response was observed) the different SSDs should not have any influence on the dose response. The effective dose rates were calculated based on a machine-set dose rate of 650 MU/min with a precise machine-set dose rate not being specified. Overall, further assessments are needed in order to qualify the use of the silicone-based dosimeter for other MRgRT systems which operate with a different magnetic field strength, machine-set dose rate or energy.

Higher sensitivity to radiation near the edges of 3D PRESAGE® and silicone dosimeters causing non-uniform dose response within the volume of the dosimeters have been reported [17,19,20]. As air-tissue interfaces are of special interest in terms of investigating the ERE, measurements of the outer layers of the dosimeters are important and we need a similar investigation of our radiochromic dosimeters in order to validate dose depositions at the boundary of air-tissue interfaces.

In this study ΔOD was defined as the mean value of $\Delta OD_{zero\text{-}dose}$ for the batch in question subtracted from $\Delta OD_{irradiated}$, whereas ΔOD usually is defined as the difference in optical density between pre- and postscans. The approach for calculating the optical response used in this study singles out the color change due to irradiation by eliminating the self-coloring of the non-irradiated dosimeters.

Fricke gels are an interesting alternative for 3D dosimetry of MRgRT systems as these dosimeters could be read out by the MRI system during or immediately after irradiation without moving the dosimeter from the treatment device to an auxiliary imaging system [21]. Compared to optical CT read-out, the Fricke dosimeter thus eliminates positioning errors associated with pre- and post-scanning, and the known limitations of diffusion-induced dose smearing for these dosimeters [22] may be of less importance for the described workflow.

In conclusion, this first study of a silicone-based radiochromic dosimeter in the presence of a magnetic field showed a linear dose response up to 22.6 Gy and no significant dose-rate dependency as a function of depth. A difference in optical response between dose delivered in one single fraction compared to multiple fractions was observed. The dosimeter showed clinical potential for dose verification in MRgRT delivery systems.

Declaration of Competing Interest

The authors declare that they have no known competing financial interests or personal relationships that could have appeared to influence the work reported in this paper.

Acknowledgment

The Novo Nordisk Foundation is gratefully acknowledged for funding of this work.

References

[1] Lee HJ, Roed Y, Venkataraman S, Carroll M, Ibbott GS. Investigation of magnetic field effects on the dose–response of 3D dosimeters for magnetic resonance – image guided radiation therapy applications. Radiother Oncol 2017;125:426–32. https://doi.org/10.1016/j.radonc.2017.08.027.

[2] Doran SJ. Radiotherapy in the presence of magnetic fields: A brief review of detector response characteristics and the contribution of 3-D measurements to the study of dose distributions at interfaces. J Phys Conf Ser 2019;1305:012006. https://doi.org/10.1088/1742-6596/1305/1/012006.

[3] Pojtinger S, Dohm OS, Kapsch RP, Thorwarth D. Ionization chamber correction factors for MR-linacs. Phys Med Biol 2018;63:11NT03. https://doi.org/10.1088/1361-6560/aac4f2.

[4] Volotskova O, Fang X, Keidar M, Chandarana H, Das IJ. Microstructure changes in radiochromic films due to magnetic field and radiation. Med Phys 2019;46:293–301. https://doi.org/10.1002/mp.13248.

[5] Barten DLJ, Hoffmans D, Palacios MA, Heukelom S, Van Battum LJ. Suitability of EBT3 GafChromic film for quality assurance in MR-guided radiotherapy at 0.35 T with and without real-time MR imaging. Phys Med Biol 2018;63:165014. https://doi.org/10.1088/1361-6560/aad58d.

[6] Park JM, Park SY, Choi CH, Chun M, Han JH, Cho JD, et al. Dosimetric characteristics of a reusable 3D radiochromic dosimetry material. PLoS ONE 2017;12:e0180970. https://doi.org/10.1371/journal.pone.0180970.

[7] Baldock C, De Deene Y, Doran S, Ibbott G, Jirasek A, Lepage M, et al. Polymer gel dosimetry. Phys Med Biol 2010;55:R1–63. https://doi.org/10.1088/0031-9155/55/5/R01.

[8] Du Y, Wang R, Wang M, Yue H, Zhang Y, Wu H, et al. Radiological tissue equivalence of deformable silicone-based chemical radiation dosimeters (FlexyDos3D). J Appl Clin Med Phys 2019;20:87–99. https://doi.org/10.1002/acm2.12658.

[9] Høye EM, Skyt PS, Yates ES, Muren LP, Petersen JBB, Balling P. A new dosimeter formulation for deformable 3D dose verification. J Phys Conf Ser 2015;573:012067. https://doi.org/10.1088/1742-6596/573/1/012067.

[10] Høye EM, Balling P, Yates ES, Muren LP, Petersen JBB, Skyt PS. Eliminating the dose-rate effect in a radiochromic silicone-based 3D dosimeter. Phys Med Biol 2015;60:5557–70. https://doi.org/10.1088/0031-9155/60/14/5557.

[11] Kaplan LP, Høye EM, Balling P, Muren LP, Petersen JBB, Poulsen PR, et al. Determining the mechanical properties of a radiochromic silicone-based 3D

dosimeter. Phys Med Biol 2017;62:5612–22. https://doi.org/10.1088/1361-6560/aa70cd.
[12] Hoye EM, Skyt PS, Balling P, Muren LP, Taasti VT, Swakoń J, et al. Chemically tuned linear energy transfer dependent quenching in a deformable, radiochromic 3D dosimeter. Phys Med Biol 2017;62:N73–89. https://doi.org/10.1088/1361-6560/aa512a.
[13] De Deene Y, Hill R, Skyt PS, Booth J. Flexydos3D: a new deformable anthropomorphic 3D dosimeter readout with optical CT scanning. J Phys Conf Ser 2015;573:012025. https://doi.org/10.1088/1742-6596/573/1/012025.
[14] De Deene Y, Skyt PS, Hil R, Booth JT. FlexyDos3D: a deformable anthropomorphic 3D radiation dosimeter: radiation properties. Phys Med Biol 2015;60:1543–63. https://doi.org/10.1088/0031-9155/60/4/1543.
[15] Höfel S, Fix MK, Zwicker F, Sterpin E, Drescher M. EPR imaging of magnetic field effects on radiation dose distributions around millimeter-size air cavities. Phys Med Biol 2019;64:175013. https://doi.org/10.1088/1361-6560/ab325b.
[16] Blaesild P, Granfeldt J. Statistics with applications in biology and geology. Boca Raton, Fla: Chapman & Hall/CRC; 2003.
[17] Wheatley MJ, Booth JT, De Deene Y. Evaporation and diffusion of chloroform with the deformable FlexyDos3D radiation dosimeter. J Phys Conf Ser 2019;1305:012044. https://doi.org/10.1088/1742-6596/1305/1/012044.
[18] Alqathami M, Blencowe A, Qiao G, Butler D, Geso M. Optimization of the sensitivity and stability of the PRESAGE^{TM} dosimeter using trihalomethane radical initiators. Radiat Phys Chem 2012;81:867–73. https://doi.org/10.1016/j.radphyschem.2012.03.022.
[19] Costa F, Doran S, Adamovics J, Nill S, Hanson IM, Oelfke U. Characterization of small PRESAGE® samples for measurements near the dosimeter edges. J Phys Conf Ser 2019;1305:012009. https://doi.org/10.1088/1742-6596/1305/1/012009.
[20] Costa F, Doran SJ, Hanson IM, Adamovics J, Nill S, Oelfke U. Edge effects in 3D dosimetry: characterisation and correction of the non-uniform dose response of PRESAGE. Phys Med Biol 2020;65:095003. https://doi.org/10.1088/1361-6560/ab7d52.
[21] Ibbott GS, Le HJ, Roe Y. The MD Anderson experience with 3D dosimetry and an MR-linac. J Phys Conf Ser 2019;1305:012011. https://doi.org/10.1088/1742-6596/1305/1/012011.
[22] Saur S, Strickert T, Wasboe E, Frengen J. Fricke gel as a tool for dose distribution verification: optimization and characterization. Phys Med Biol 2005;50:5251–61. https://doi.org/10.1088/0031-9155/50/22/003.